

Modern Physics Letters A
 © World Scientific Publishing Company

LEPTON FLAVOR VIOLATION IN INVERSE SEESAW MODEL

KE-SHENG SUN ^{a,b,*}, TAI-FU FENG ^b, GUO-HUI LUO ^a, XIU-YI YANG ^{c,d},
 JIAN-BIN CHEN ^e

^a *Department of Physics, Dalian University of Technology, Dalian 116024, China*

^b *Department of Physics, Hebei University, Baoding 071002, China*

^c *School of Physics, Shandong University, Jinan 250100, China*

^d *School of Science, University of Science and Technology Liaoning, Anshan 114051, China*

^e *College of Physics and Optoelectronics, Taiyuan University of Technology, Taiyuan 030024, China*

* *sunkesheng@126.com*

Received (Day Month Year)

Revised (Day Month Year)

We analyze the lepton flavor violation processes $\mu - e$ conversion, $l_i \rightarrow l_j \gamma$ and $l_i \rightarrow 3l_j$ in framework of the Standard Model (SM) extended with inverse seesaw mechanism, as a function of $\tilde{\eta} = 1 - |Det(\tilde{U}_{PMNS})|$ that parameterizes the departure from unitary of the light neutrino mixing sub-matrix \tilde{U}_{PMNS} . In a wide range of $\tilde{\eta}$, the predictions on the $\mu - e$ conversion rates and the branching ratio of $\mu \rightarrow e \gamma$ are sizeable to be compatible with the experimental upper limits or future experimental sensitivities. For large scale of $\tilde{\eta}$, the predictions on branching ratios of other lepton flavor processes can also be reach the experimental upper limits or future experimental sensitivities. The value of $\tilde{\eta}$ depends on the determinant of the Majorana mass term M_μ . Finally, searching for lepton flavor violation processes in experiment provides us more opportunities for the searches of seesaw nature of the neutrino masses.

Keywords: Lepton flavor violating; Inverse seesaw; Non-unitary.

1. Introduction

Neutrino oscillation experiments ^{1,2,3,4} have established compelling evidence that neutrinos are massive and the neutral lepton flavor is not conserved. In SM extended with massive neutrinos, the charged Lepton Flavor Violation (LFV) processes, arising from loop level, such as radiative two body decays ($l_i \rightarrow l_j \gamma$) and leptonic three body decays ($l_i \rightarrow 3l_j$), remain highly suppressed, see Table.1⁵ for current experimental upper bounds, making them difficult to observe. The limit on branching ratio of $\mu \rightarrow e \gamma$ is the most recent result given by the MEG experiments at the 90% confidence level ⁶. Nevertheless, various extensions of the SM, such as the seesaw model with or without GUT, supersymmetry, Z' models, etc., have predicted enhanced branching ratios of LFV processes to be accessible in current experiments. Thus, searching for LFV processes are a powerful way to prove physics beyond the SM.

Table 1. Current limits and future expectations for $\mu - e$ conversion, $l_i \rightarrow l_j \gamma$ and $l_i \rightarrow 3l_j$.

Channel	Limit	Future
$CR(\mu - e, Al)$	-	$2.4 \times 10^{-17}, 7, 10^{-17}, 8$
$CR(\mu - e, Ti)$	$< 4.3 \times 10^{-12}$	$10^{-18}, 9$
$CR(\mu - e, SiC)$	-	$10^{-14}, 10$
$CR(\mu - e, Au)$	$< 7 \times 10^{-13}$	-
$CR(\mu - e, Pb)$	$< 4.6 \times 10^{-11}$	-
$BR(\mu \rightarrow e \gamma)$	$< 5.7 \times 10^{-13}$	$6 \times 10^{-14}, 11$
$BR(\tau \rightarrow e \gamma)$	$< 3.3 \times 10^{-8}$	$2.3 \times 10^{-9}, 12$
$BR(\tau \rightarrow \mu \gamma)$	$< 4.4 \times 10^{-8}$	$3 \times 10^{-9}, 13, 1.8 \times 10^{-9}, 12$
$BR(\mu \rightarrow 3e)$	$< 1.0 \times 10^{-12}$	$10^{-15}, 14, 10^{-16}, 15$
$BR(\tau \rightarrow 3e)$	$< 2.7 \times 10^{-8}$	$2 \times 10^{-10}, 12$
$BR(\tau \rightarrow 3\mu)$	$< 2.1 \times 10^{-8}$	$10^{-9}, 13, 2 \times 10^{-10}, 12$

The seesaw mechanisms have been recognized as the most natural scenario for understanding the smallness of neutrino mass up to now. In canonical Type(I) seesaw, three right-handed neutrinos are introduced, and to achieve sub-eV range of light neutrino masses, Grand Unified (GUT) scale (i.e., 10^{16} GeV) of the right-handed neutrinos is required and that makes the LHC study of the new physics scale difficult. In order to make the right-handed neutrino masses down to the TeV scale, the small neutrino masses have to be effectively suppressed via other mechanisms rather than the GUT scale, such as radiative generation, small lepton number breaking, or neutrino masses from a higher than dimension-five effective operator¹⁶. Another option to relate small neutrino mass to TeV scale physics is the inverse seesaw mechanism^{17,18}. The smallness of the light neutrino masses can be ascribed to the smallness of M_μ , which breaks the lepton number by two unity.

The smallness of M_μ is a key element of the inverse seesaw models. So far, a very appealing picture is the radiative origin of the two unity lepton number-breaking parameter as it has been proposed in Ref.19: it is induced at two-loop level, thus explaining its smallness with respect to the electroweak scale (EW). Introducing new scalar fields, the two unity lepton number-breaking term can also be induced at two-loop level and is naturally around the keV scale, while righthanded neutrinos are at the TeV scale²⁰. In the supersymmetric inverse seesaw mechanism, the smallness of M_μ was related to vanishing trilinear susy soft terms at the grand unified theory (GUT) scale²¹. In warped extra dimension, one can have the M_μ smallness dictated by parameters of order one that govern the location of the 5D profile of the S fields in the bulk²².

The effective mass matrix for the light neutrinos is given by

$$m_\nu \approx M_D^T (M_R^T)^{-1} M_\mu (M_R)^{-1} M_D. \quad (1)$$

So that scale of M_R can be made small and many phenomena due to the non-unitary feature of the neutrino mixing matrix can be manifested, such as LFV, CP violation and non standard effects in neutrino propagation²³. Non-unitary mixing between

light and heavy particles can be large and can be probed at colliders ^{24,25,26,27} and future neutrino factories ^{28,29,30}.

The LFV effect of the non-unitary feature of the neutrino mixing matrix have been investigated in several literatures where the inverse seesaw mechanism is accommodated in SM ^{23,31,32,33,34}, SM with B - L extension ³⁵ and supersymmetric models ^{36,37,38,39}. It is shown that LFV decay $\mu \rightarrow e\gamma$ can be sizeable to be observed in experiment, where the scale of M_R is fixed to 10^3 GeV and the scale of M_μ varies in the range of $[10^{-10}, 10^{-8}]$ GeV, and to be compatible with the experiment limit on $\mu \rightarrow e\gamma$, large value setup of M_μ is favored ²³. Assuming $\Delta L = 2$ interactions are absent from the model, i.e., $M_\mu = 0$, Ref.31 estimate the $BR(\tau \rightarrow 3e)$ or $BR(\tau \rightarrow e\mu\mu)$ can be large as 10^{-6} and the limits are out of date. In the inverse seesaw model, the limits on degenerate values of M_R and M_μ from the photonic contribution are much more stringent than from the non-photonic contribution for $\mu - e$ conversion in nucleus, and the rates arising from virtual photon exchange are generically correlated to the $\mu \rightarrow e\gamma$ decay ³⁴. It is also shown that prediction on the branching ratio of $\mu \rightarrow e\gamma$ can be within the reach of MEG experiment in B - L extension of the SM with inverse seesaw mechanism ³⁵. In supersymmetric inverse seesaw model, the LFV decays can be enhanced by flavour violating slepton contributions, the non-unitary of the charged current mixing matrix or the Higgs mediated processes ^{36,37,38}. In the framework of a supersymmetric $SO(10)$ model with inverse seesaw ³⁹, the expected branching ratio for $(l_i \rightarrow l_j\gamma)$ are several orders of magnitude below the future sensitivity in experiment with TeV scale slepton mass, and for $(l_i \rightarrow 3l_j)$ and $\mu - e$ conversion, the predictions are much smaller than what can be probed in planned experiments.

In SM, the LFV decays mainly originate from the charged current with the mixing among three lepton generations. The fields of the flavor neutrinos in charged current weak interaction Lagrangian are combinations of three massive neutrinos:

$$\mathcal{L} = -\frac{g_2}{\sqrt{2}} \sum_{l=e,\mu,\tau} \bar{l}_L(x) \gamma_\mu \nu_{lL}(x) W^\mu(x) + h.c.,$$

$$\nu_{lL}(x) = \sum_{i=1}^3 \left(U_{PMNS} \right)_{li} \nu_{iL}(x), \quad (2)$$

where g_2 denotes the coupling constant of gauge group SU(2), ν_{lL} are fields of the flavor neutrinos, ν_{iL} are fields of massive neutrinos, and U_{PMNS} corresponds to the unitary neutrino mixing matrix ^{40,41,42}.

In this paper we have studied LFV decays $l_i \rightarrow l_j\gamma$, $l_i \rightarrow 3l_j$ and $\mu - e$ conversion as a function of non-unitary parameter $\tilde{\eta}$, which is firstly introduced in Ref.43 in the SM extended with inverse seesaw mechanism. Moreover, we also investigate the dependence of $\tilde{\eta}$ on M_μ . From this point of view, the paper proposed is different from others. We perform a scan over non-degenerate parameters M_R and M_μ , which vary in region of $[1, 10^6]$ GeV and $[10^{-11}, 10^{-3}]$ GeV, respectively, by taking account of the constraints from neutrino oscillation data and several rare decays. We have

4 *Ke-Sheng Sun, etc.*

give a discussion about the parameter spaces, which is more narrow than Ref.34. For $CR(\mu - e, Nucleus)$, both photonic and non-photonic contribution are considered in this paper.

The paper is organized as follows. In Section.2, we review the inverse seesaw mechanism and give the expressions for the unitary violating parameter $\tilde{\eta}$. The numerical results and discussions are presented in Section.3. The conclusion is drawn in Section.4.

2. Inverse seesaw model

The inverse seesaw mechanism can be accommodated in SM by adding two kind of singlet fermions, N_R^i and S_R^i , and one gauge singlet scalar Φ to the SM field content, where N_R^i ($i = 1, 2, 3$) stand for the usual right-handed neutrinos, S_R^i ($i = 1, 2, 3$) stand for the additional gauge singlet neutrinos, and these two kind fermions share opposite lepton number (-1 and 1, respectively). The relevant gauge invariant Lagrangian for neutrino masses is given by ^{17,18,20,44}:

$$\mathcal{L} = \overline{N_R^c} Y_\nu \tilde{H} l_L + \overline{N_R^c} Y'_\nu S_R \Phi + \frac{1}{2} \overline{S_R^c} M_\mu S_R + h.c., \quad (3)$$

where l_L stands for the $SU(2)_L$ lepton doublet, $\tilde{H} \equiv i\sigma_2 H^*$ stands for the Higgs doublets, Y_ν and Y'_ν are the 3×3 Yukawa coupling matrices, and M_μ is a symmetric Majorana mass matrix. In this mechanism, it introduces an extra $U(1)$ gauge symmetry into the electroweak model, under which the right-handed neutrino must be a non-singlet. After spontaneous gauge symmetry breaking, the extra $U(1)$ gauge group breaks into $U(1)_Y$, the weak hypercharge of the standard model. The invariant Lagrangian in Eq.(3) would be:

$$\mathcal{L} = \overline{\nu_L} M_D N_R^c + \overline{N_R^c} M_R S_R + \frac{1}{2} \overline{S_R^c} M_\mu S_R + h.c., \quad (4)$$

where $M_D = Y_\nu \langle H \rangle = \frac{v}{\sqrt{2}} Y_\nu$ and $M_R = Y'_\nu \langle \Phi \rangle$ are 3×3 mass matrices, with v the vacuum expectation value of the SM Higgs boson. It shows that the right-handed neutrino mass term M_R conserves lepton number and the Majorana mass term M_μ violates the lepton number by two units.

The neutrino mass matrix in the flavor basis defined by (ν_L, N_R^c, S_R^c) is given by

$$\mathcal{M} = \begin{pmatrix} 0 & M_D^T & 0 \\ M_D & 0 & M_R \\ 0 & M_R^T & M_\mu \end{pmatrix}, \quad (5)$$

where \mathcal{M} is a 9×9 matrix. The mass scales of M_D, M_R and M_μ in Eq.(5) may naturally have a hierarchy $M_R \gg M_D \gg M_\mu$ ⁴⁵. In reality, a small non-vanishing M_μ can be viewed as a slight breaking of a global $U(1)$ symmetry. The 9×9 neutrino mass matrix \mathcal{M} can be diagonalized by the unitary mixing matrix U :

$$\hat{\mathcal{M}} = U^T \mathcal{M} U, \quad (6)$$

and it yields nine mass eigenstates N_i . The light neutrino flavour states ν_{lL} could be given in terms of the mass eigenstates via the unitary matrix U as

$$\nu_{lL} = \sum_{i=1}^9 (U)_{li} N_i. \quad (7)$$

It is obvious that the mixing matrix would be simply the rectangular matrix formed by the first three rows of U in Eq.(6) and the matrix \tilde{U}_{PMNS} describing the mixing between the charged leptons and light neutrinos in inverse seesaw mechanism could be written by:

$$\tilde{U}_{PMNS} = \begin{pmatrix} U_{11} & U_{12} & U_{13} \\ U_{21} & U_{22} & U_{23} \\ U_{31} & U_{32} & U_{33} \end{pmatrix}. \quad (8)$$

In inverse seesaw mechanism, U in Eq.(6) is unitary. However, \tilde{U}_{PMNS} is not unitary. To parametrize this departure from unitarity, we could define $\tilde{\eta}$ as in Ref.43 by:

$$\tilde{\eta} = 1 - |Det(\tilde{U}_{PMNS})|. \quad (9)$$

It has been shown in Ref.43 that large value of $\tilde{\eta}$ is responsible for the lepton flavour universality violation in K^+ and π^+ leptonic decays in SM extended with inverse seesaw mechanism.

The diagonalization of \mathcal{M} leads to an effective mass matrix for the light neutrinos in the leading order approximation ⁴⁶,

$$m_\nu = M_D^T (M_R^T)^{-1} M_\mu (M_R)^{-1} M_D, \quad (10)$$

which indicates that the light neutrino masses vanish in the limit $M_\mu \rightarrow 0$ and lepton number conservation is restored. The effective mass matrix m_ν is diagonalized by the physical neutrino mixing matrix U_{PMNS} ,

$$\hat{m}_\nu = U_{PMNS}^T m_\nu U_{PMNS}, \quad (11)$$

and, in the standard parametrization ⁵, U_{PMNS} is given by

$$U_{PMNS} = \begin{pmatrix} c_1 c_3 & c_3 s_1 & s_3 e^{-i\delta} \\ -c_1 s_3 s_2 e^{i\delta} - c_2 s_1 & c_1 c_2 - s_1 s_2 s_3 e^{i\delta} & c_3 s_2 \\ s_1 s_2 - c_1 s_3 c_2 e^{i\delta} & c_1 s_2 - s_1 c_2 s_1 e^{i\delta} & c_3 c_2 \end{pmatrix} \\ \times \text{diag}(e^{i\Phi_1/2}, 1, e^{i\Phi_2/2}), \quad (12)$$

where $s(c)_1 = \sin(\cos)\theta_{12}$, $s(c)_2 = \sin(\cos)\theta_{23}$, $s(c)_3 = \sin(\cos)\theta_{13}$, and the experimental limits on the mixing angles are given in Table.2. The phase δ is the Dirac CP phase, and Φ_i are the Majorana phases. The remaining six heavy states have masses approximately given by $M_\nu \simeq M_R$.

Without loss of generality, we work in a basis where M_R is assumed as diagonal matrix. Using a modified Casas-Ibarra parametrisation ⁴⁷, which is automatically reproducing the light neutrino data, Y_ν can be written by

$$Y_\nu = \frac{\sqrt{2}}{v} V^\dagger \sqrt{\hat{M} R} \sqrt{\hat{m}_\nu} U_{PMNS}^\dagger, \quad (13)$$

6 *Ke-Sheng Sun, etc.*

with v the vacuum expectation value of the SM Higgs boson. \hat{M} is the relevant diagonal matrix of $M = M_R M_\mu^{-1} M_R^T$, which is diagonalized by matrix V :

$$\hat{M} = V M V^T = V M_R M_\mu^{-1} M_R^T V^T, \quad (14)$$

and R is a 3×3 complex orthogonal matrix, parametrized by three complex angles $\alpha_1, \alpha_2, \alpha_3$:

$$R = \begin{pmatrix} c_2 c_3 & -c_1 s_3 - s_1 s_2 c_3 & s_1 s_3 - c_1 s_2 c_3 \\ c_2 s_3 & c_1 c_3 - s_1 s_2 s_3 & -s_1 c_3 - c_1 s_2 s_3 \\ s_2 & s_1 c_2 & c_1 c_2 \end{pmatrix}, \quad (15)$$

with the notation $c_i = \cos \alpha_i$ and $s_i = \sin \alpha_i$, with $i = 1, 2, 3$. For simplify, we will assume R is real in our calculation.

The interactions of the nine neutrino mass eigenstates, $N_{i,j}$, and charged leptons, l_i , with the gauge bosons, W^\pm and Z , are correspondingly given by the Lagrangians:

$$\mathcal{L}^{W^\pm} = \frac{g_2}{\sqrt{2}} U_{ij} \bar{l}_i \gamma^\mu P_L N_j W_\mu^\pm + h.c., (i = 1, \dots, 3, j = 1, \dots, 9), \quad (16)$$

$$\mathcal{L}^Z = \frac{g_2}{2c_w} C_{ij} \bar{N}_i \gamma^\mu P_L N_j Z_\mu, (i, j = 1, \dots, 9), \quad (17)$$

where g_2 is the coupling constant of gauge group $SU(2)$, and c_w is the cosine of the weak mixing angle. $P_{L/R} = \frac{1}{2}(1 \mp \gamma_5)$. C_{ij} is defined as

$$C_{ij} = \sum_{\alpha=1}^3 U_{i\alpha}^\dagger U_{\alpha j}. \quad (18)$$

Here, C_{ij} is also not unitary.

3. Numerical Analysis

To quantitatively study the non-unitary effect on various LFV processes, we perform a scan over the parameter space described as following.

Before the calculation, it is clear that present data on neutrino masses and mixing should be accounted for, which are listed in Table.2⁵.

Table 2. Neutrino oscillation data from PDG.

Parameter	Value	Parameter	Value
$\sin^2 2\theta_{12}$	0.857 ± 0.024	Δm_{21}^2	$(7.50 \pm 0.20) \times 10^{-5} eV^2$
$\sin^2 2\theta_{23}$	> 0.95	$ \Delta m_{32}^2 $	$(0.00232_{-0.00008}^{+0.00012}) eV^2$
$\sin^2 2\theta_{13}$	0.098 ± 0.013		

In calculation, we have randomly varied the values of $\sin^2 2\theta_{12}$, $\sin^2 2\theta_{13}$, Δm_{21}^2 and Δm_{32}^2 within 3σ experimental errors and set the value of $\sin^2 2\theta_{23}$ equal to 1. The light neutrino mass spectrum is assumed to be normal ordering, i.e., $\Delta m_{32}^2 > 0$, and CP violating phases δ , Φ_1 and Φ_2 are set to zero. The lightest neutrino mass

would vary in region of $[10^{-5}, 1]$ eV. We also assume the R matrix angles in Eq.(15) are taken to be real (thus no contributions to lepton electric dipole moments are expected), and randomly vary in the range $[0, 2\pi]$. The use of Y_ν in Eq.(13) ensures us the above neutrino oscillation data satisfied.

In SM with inverse seesaw mechanism, the relevant input parameters are the right-handed neutrino mass matrix M_R and Majorana mass matrix M_μ . Here, as mentioned before Eq.(13), M_R is diagonal matrix. We will make the minimal flavor violation hypothesis which consists in assuming that flavor is violated only in the standard Dirac Yukawa coupling. Under this simplification the 3×3 matrix M_μ must be also diagonal. We have randomly varied the entries of $(M_R)_{ii}$ in the range of $[1, 10^6]$ GeV and $(M_\mu)_{ii}$ in the range of $[10^{-11}, 10^{-3}]$ GeV.

Table 3. Constraints used in the scan over free parameters.

Channel	Fraction or Limit	Channel	Fraction or Limit
$W \rightarrow e\nu$	0.1075 ± 0.0013	$W \rightarrow \mu\nu$	0.1057 ± 0.0015
$W \rightarrow \tau\nu$	0.1125 ± 0.0020	$B \rightarrow e\nu$	$< 9.8 \times 10^{-7}$
$B \rightarrow \tau\nu$	$(1.65 \pm 0.34) \times 10^{-4}$	$B \rightarrow \mu\nu$	$< 1.0 \times 10^{-6}$
$D_s \rightarrow \mu\nu$	$(5.90 \pm 0.33) \times 10^{-3}$	$D_s \rightarrow e\nu$	$< 1.2 \times 10^{-4}$
$D_s \rightarrow \tau\nu$	$5.43 \pm 0.31\%$	$\pi \rightarrow e\nu$	$(1.230 \pm 0.004) \times 10^{-8}$
$K \rightarrow \mu\nu$	0.6355 ± 0.0011	$\pi \rightarrow \mu\nu$	$99.98770 \pm 0.00004\%$
$K \rightarrow e\nu$	$(1.581 \pm 0.008) \times 10^{-5}$	$Z \rightarrow \mu\tau$	$< 1.2 \times 10^{-5}$
$Z \rightarrow e\mu$	$< 1.7 \times 10^{-6}$	$Z \rightarrow e\tau$	$< 9.8 \times 10^{-6}$

The experimental measurements of several rare decays should be also considered cause the parameter spaces are strongly constrained by such measurements. These rare decays have been investigated in literatures^{31,32,43,48}. The non-unitary nature of the neutrino mixing matrix can manifest itself in tree level processes like leptonic decays of W boson and mesons (B^+, D_s^+, K^+ and π^+), and invisible decay of Z boson. It can also manifest in LFV decays of Z boson, LFV rare charged lepton decays like $l_i \rightarrow l_j \gamma$, $l_i \rightarrow 3l_j$, and LFV process $\mu - e$ conversion in an atom, which proceed via one loop processes, and hence can be constrained. The current experimental limits are listed in Table.1 and Table.3 at 1σ level. Current experimental limits are listed at the 90% confidence level⁵(except for $Z \rightarrow e^\pm \mu^\pm$, $Z \rightarrow e^\pm \tau^\pm$ and $Z \rightarrow \mu^\pm \tau^\pm$ for which the 95% C.L bounds are given). We will use these limits to bound the parameter spaces. For the channels listed in Table.3, we require that our numerical results are compatible with the experimental values within 3σ experimental errors.

We have studied the possible constraints on the mass matrix inputs $(M_R)_{11}$, $(M_R)_{22}$, $(M_R)_{33}$, $(M_\mu)_{11}$, $(M_\mu)_{22}$ and $(M_\mu)_{33}$. It has been studied in Ref.34 that the region of $\frac{M_\mu}{M_R} \lesssim 10^{-7}$ has been excluded by considering the constraints from $\mu - e$ conversion in various nucleus, where the eigenvalues of both M_R and M_μ are degenerate. We display the area plot of $\frac{(M_\mu)_{11}}{(M_R)_{11}}$ versus $(M_R)_{11}$ in Fig.1. It shows that, without the assumption the eigenvalues of both M_R and M_μ are degenerate and by considering more constraints, the excluded region is narrowed to $\frac{M_\mu}{M_R} \lesssim 10^{-9}$. In

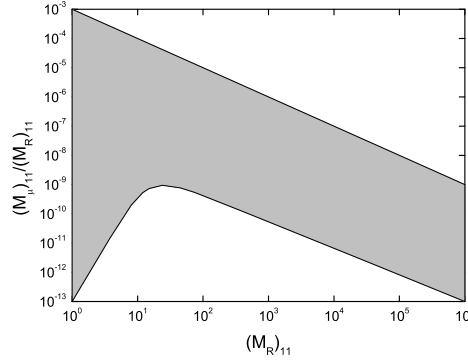


Fig. 1. Area plot of $\frac{(M_\mu)_{11}}{(M_R)_{11}}$ versus $(M_R)_{11}$. The shadow region is compatible with constraints in Table.1 and Table.3.

addition, the blank area in the upper right corner in Fig.1 is also excluded, which is not displayed in Ref.34. With fixed value of the scale of M_R to 10^3 GeV, the lower value of the scale of M_μ is approximately given by $M_\mu \sim 10^{-9}$ or $\frac{M_\mu}{M_R} \sim 10^{-12}$ in Ref.23 by considering the constraint from $\mu \rightarrow e\gamma$, which is also less restrictive than our result. There are similar correlations for $\frac{(M_\mu)_{22}}{(M_R)_{22}}$ versus $(M_R)_{22}$ and $\frac{(M_\mu)_{33}}{(M_R)_{33}}$ versus $(M_R)_{33}$, which are not displayed to shorten the length of text.

We also investigate the dependence of $\tilde{\eta}$ on $\sin^2 2\theta_{12}$, $\sin^2 2\theta_{13}$, Δm_{21}^2 , Δm_{32}^2 , m_{ν_e} , $(M_R)_{ii}$ and $(M_\mu)_{ii}$. It displays $\tilde{\eta}$ strongly depends on $(M_\mu)_{ii}$. In Fig.2, we display the determinant $Det(M_\mu)$ versus $Log[\tilde{\eta}]$ from a scan over few 10^6 points in parameter space in the inverse seesaw mechanism. Here, $Det(M_\mu) = \prod_{i=1}^3 (M_\mu)_{ii}$. It shows that large values of unitary violation $\tilde{\eta}$ (e.g., 10^{-4}) correspond to small scales of $Det(M_\mu)$ (e.g., 10^{-15} GeV³) or $(M_\mu)_{ii}$ (e.g., 10^{-5} GeV). In models where lepton number is spontaneously broken by a vacuum expectation value $\langle \sigma \rangle$ ⁴⁶ one has $(M_\mu)_{ii} = (\lambda)_{ii} \langle \sigma \rangle$, where M_μ is diagonal as assumed. For typical Yukawas $(\lambda)_{ii} \sim 10^{-3}$ one sees that $(M_\mu)_{ii} \sim 10^{-6}$ GeV corresponds to a scale of lepton number violation value $\langle \sigma \rangle \sim 10^{-3}$ GeV³⁴. Thus, if the LFV processes are observed in experiment, the vacuum expectation value $\langle \sigma \rangle$ should be the scale of $(1 - 10^{-3})$ GeV, under the assumption of typical Yukawas.

In Fig.3, we show the area plot of $CR(\mu - e, Au)$ versus $Log[\tilde{\eta}]$ in the inverse seesaw mechanism from the scan over few 10^6 points in parameter space. The expected conversion rates $CR(\mu \rightarrow e, Au)$ are sizeable to compatible with the experimental upper limit and future experimental sensitivities in range of $10^{-14} < \tilde{\eta} < 10^{-4}$. For $\tilde{\eta} < 10^{-14}$, the upper limit of the $CR(\mu - e, Au)$ decreases. The expected conversion rates $CR(\mu \rightarrow e, Au)$ could be very small in the whole region of $10^{-18} < \tilde{\eta} < 10^{-4}$. The area plots for $CR(\mu - e, Al)$, $CR(\mu - e, Ti)$ and $CR(\mu - e, Pb)$ versus $Log[\tilde{\eta}]$ have the same behavior.

In Fig.4, we display area plot of $BR(\mu \rightarrow e\gamma)$ and $BR(\tau \rightarrow e\gamma)$ versus $Log[\tilde{\eta}]$

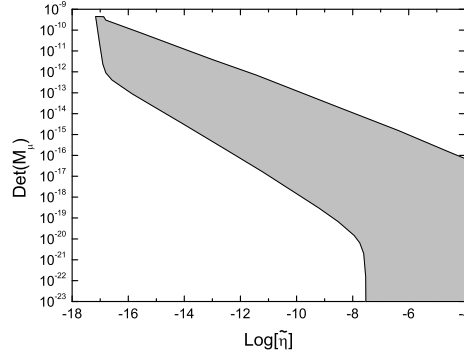


Fig. 2. Area plot of $\text{Det}(M_\mu)$ versus $\text{Log}[\tilde{\eta}]$. The shadow region is compatible with constraints in Table.1 and Table.3.

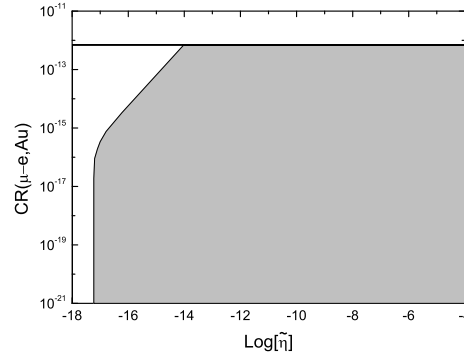


Fig. 3. Area plot of $CR(\mu - e, Au)$ versus $\text{Log}[\tilde{\eta}]$. The horizontal solid line denotes the experimental bound. The shadow region is compatible with constraints in Table.1 and Table.3.

in the inverse seesaw mechanism from the scan over few 10^6 points in parameter space. It shows most predictions of $BR(\mu \rightarrow e\gamma)$ are just below the experimental upper limit in range of $10^{-16} < \tilde{\eta} < 10^{-4}$. In a narrow range of $10^{-18} < \tilde{\eta} < 10^{-16}$, the upper limit of the predictions decreases. The prediction of $BR(\tau \rightarrow e\gamma)$ can reach to the current limits only when $\tilde{\eta}$ is large ($\tilde{\eta} > 10^{-10}$). The upper limit of the predictions decreases when $\tilde{\eta} < 10^{-10}$. It is noteworthy that $\mu \rightarrow e\gamma$ is more constraining than $\tau \rightarrow e\gamma$ in most cases from a compare between figures in Fig.4. However, there is still probability that both predictions of these processes are very close to the experimental upper limit ($\tilde{\eta} > 10^{-10}$). The area plot for $BR(\tau \rightarrow \mu\gamma)$ versus $\text{Log}[\tilde{\eta}]$ has the same behavior with $BR(\tau \rightarrow e\gamma)$ versus $\text{Log}[\tilde{\eta}]$.

In Fig.5, we display area plot of $BR(\mu \rightarrow 3e)$ and $BR(\tau \rightarrow 3e)$ versus $\text{Log}[\tilde{\eta}]$ in the inverse seesaw mechanism. It displays that the predictions of $BR(\mu \rightarrow 3e)$ and

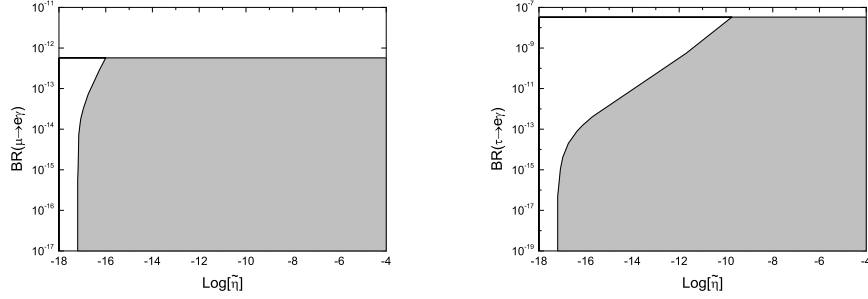


Fig. 4. Area plot of $BR(\tau \rightarrow e\gamma)$ versus $\text{Log}[\tilde{\eta}]$ and $BR(\mu \rightarrow e\gamma)$ versus $\text{Log}[\tilde{\eta}]$. The horizontal solid line denotes the experimental bound. The shadow region is compatible with constraints in Table.1 and Table.3.

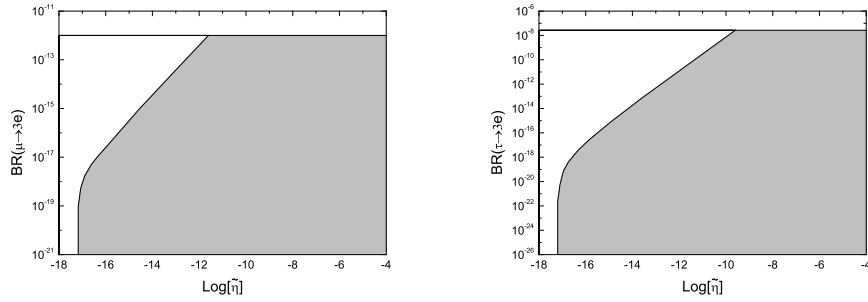


Fig. 5. Area plot of $BR(\tau \rightarrow 3e)$ versus $\text{Log}[\tilde{\eta}]$ and $BR(\mu \rightarrow 3e)$ versus $\text{Log}[\tilde{\eta}]$. The horizontal solid line denotes the experimental bound. The shadow region is compatible with constraints in Table.1 and Table.3.

$BR(\tau \rightarrow 3e)$ can reach the experimental limit at large values of $\tilde{\eta}$ (about $\tilde{\eta} > 10^{-12}$ and $\tilde{\eta} > 10^{-10}$). Also, the upper limits of predictions decrease when $\tilde{\eta} < 10^{-12}$ and $\tilde{\eta} < 10^{-10}$, respectively. The observation of LFV decays $\mu \rightarrow 3e$ and $\tau \rightarrow 3e$ indicate the large violation of unitary in light neutrino mixing matrix and a lower vacuum expected value $\langle\sigma\rangle$. The area plot for $BR(\tau \rightarrow 3\mu)$ versus $\text{Log}[\tilde{\eta}]$ has the same behavior with $BR(\tau \rightarrow 3e)$ versus $\text{Log}[\tilde{\eta}]$.

4. Conclusions

The non-unitary mixing matrix in seesaw mechanism is a generic feature for theories with mixing between neutrinos and heavy states and provides a window to probe new physics at TeV scale.

In this paper we have studied lepton flavor violation decays $l_i \rightarrow l_j\gamma$, $l_i \rightarrow 3l_j$ and $\mu - e$ conversion as a function of non-unitary parameter $\tilde{\eta}$ in the SM extended

with inverse seesaw mechanism through a scan over the parameter spaces defined from the right-handed neutrino mass matrix M_R and Majorana mass matrix M_μ . Taking account of the constraints from neutrino oscillation and various rare decays, the relevant parameter spaces are more narrow than that in Ref.34. The result shows that large values of unitary violation $\tilde{\eta}$ are related to small scales of $\text{Det}(M_\mu)$ or a small vacuum expectation value $\langle\sigma\rangle$ in spontaneously lepton number broken models. In range of $10^{-14} < \tilde{\eta} < 10^{-4}$, the upper limits of predictions of $CR(\mu-e, \text{Nucleus})$ and $BR(\mu \rightarrow e\gamma)$ can reach the sensitivity of experiment, and is promising to detect directly in experiment in near future. In range of $10^{-10} < \tilde{\eta} < 10^{-4}$, the upper limits of $BR(\tau \rightarrow e(\mu)\gamma)$, $BR(\mu \rightarrow 3e)$ and $BR(\tau \rightarrow 3e(\mu))$ can also reach the sensitivity of experiment. Finally, searching for LFV processes can serve as a window to the new physics of seesaw nature of neutrino masses.

Acknowledgements

The work has been supported by the National Natural Science Foundation of China (NNSFC) with Grants No.11275036 and 11047002 and Natural Science Fund of Hebei University with Grant No. 2011JQ05, No. 2012-242.

References

1. Y. Fukuda et al., Phys. Lett. **B335**(1994)237.
2. Y. Fukuda et al., Phys. Rev. Lett.**81**(1998)1562.
3. Q. R. Ahmad et al., Phys. Rev. Lett.**89**(2002)011301.
4. K. Eguchi et al., Phys. Rev. Lett.**90**(2003)021802.
5. J. Beringer et al. (Particle Data Group), Phys. Rev. D**86**(2012)010001.
6. J. Adam et al. [MEG Collaboration], hep-ex/1303.0754.
7. R. J. Abrams et al. [Mu2e Collaboration], arXiv:1211.7019 [physics.ins-det].
8. Y. Kuno, Nucl. Phys. Proc. Suppl. **225**(2012) 228.
9. R. J. Barlow, "The PRISM/PRIME project," Nucl. Phys. Proc. Suppl.**218**(2011)44.
10. M. Aoki [DeeMe Collaboration], AIP Conf. Proc. **1441**(2012) 599.
11. J. Adam et al. [MEG Collaboration], arXiv:1301.7225[physics.ins-det].
12. M. Bona et al.[SuperB Collaboration].hep-ph/0709.0451.
13. T. Abe. et al. (Belle II).hep-ph/1011.0352.
14. M. Yoshida, "The MUSIC Project," AIP Conf. Proc. **1222**(2010)400.
15. A. Blondel et al., "Letter of Intent for an Experiment to Search for the Decay $\mu \rightarrow 3e$," <http://www.physi.uni-heidelberg.de/Forschung/he/mu3e/>, (2012).
16. F. Bonnet, D. Hernández, T. Ota, and W. Winter, JHEP**10**(2009)076.
17. R. N. Mohapatra and J. W. F. Valle, Phys. Rev. D**34**(1986)1642.
18. R. N. Mohapatra, Phys. Rev. Lett.**56**(1986)561.
19. E. Ma, Phys. Rev. D **80**, 013013 (2009).
20. Federica Bazzocchi. Phys. Rev. D**83**(2011)093009.
21. F. Bazzocchi, D. G. Cerdeno, C. Munoz, and J.W. F. Valle, Phys. Rev. D **81**, 051701 (2010).
22. Chee Sheng Fong, Rabindra N. Mohapatra and Ilmo Sung. Phys. Lett. B **704**(2011)171.
23. D.V. Forero, S. Morisi, M.Tortola and J.W.F. Valle.JHEP**09**(2011)142.

12 *Ke-Sheng Sun, etc.*

24. ISS Physics Working Group collaboration, A. Bandyopadhyay et al., Rep. Prog. Phys. **72**(2009)106201.
25. A. Das and N. Okada, arXiv:1207.3734.
26. P. S. B. Dev, R. Franceschini and R. N. Mohapatra. Phys. Rev. D **86** (2012) 093010.
27. P. Bandyopadhyay, E. J. Chun, H. Okada and J. -C. Park. JHEP **1301** (2013) 079.
28. E. Fernandez-Martinez, M. B. Gavela, J. Lopez-Pavon and O. Yasuda, Phys. Lett. B **649** (2007) 427.
29. S. Goswami and T. Ota, Phys. Rev. D **78**, 033012 (2008).
30. S. Antusch, M. Blennow, E. Fernandez-Martinez and J. Lopez-Pavon, Phys. Rev. D **80**, 033002 (2009).
31. A. Ilakovac and A. Pilaftsis, Nucl. Phys. B **437**(1995)491.
32. S. Antusch, C. Biggio, E. Fernandez-Martinez, M.B. Gavela, J. Lopez-Pavon. JHEP **10**(2006)084.
33. R. Alonso, M. Dhen, M. B. Gavela and T. Hambye, hep-ph/1209.2679.
34. F. Deppisch, T. S. Kosmas, J. W. F. Valle. Nucl. Phys. B **752**(2006)80.
35. W. Abdallah, A. Awad, S. Khalil, H. Okada. Eur. Phys. J. C **72**(2012)2108.
36. F. Deppisch and J. Valle. Phys. Rev. D **72**(2005)036001.
37. A. Abada, D. Das, A. Vicente and C. Weiland. JHEP **09**(2011)015.
38. A. Abada, D. Das and C. Weiland. JHEP **03**(2012)100.
39. P. S. Bhupal Dev and R. N. Mohapatra. Phys. Rev. D **81**(2010)013001
40. B. Pontecorvo, Zh. Eksp. Teor. Fiz. JETP **33**(1957)549.
41. B. Pontecorvo, Zh. Eksp. Teor. Fiz. JETP **34**(1958)247.
42. Z. Maki, M. Nakagawa and S. Sakata, Prog. Theor. Phys. **28**(1962)870.
43. A. Abada, D. Das, A.M. Teixeira, A. Vicente and C. Weiland. JHEP **02**(2013)048.
44. Aik Hui Chan, Hwee Boon Low, Zhi-zhong Xing. Phys. Rev. D **80**(2009)073006.
45. G. t Hooft, in Proceedings of 1979 Cargese Institute on Recent Developments in Gauge Theories, edited by G. t Hooft et al. (Plenum Press, New York, 1980), p. 135.
46. M. C. Gonzalez-Garcia, J. W. F. Valle, Phys. Lett. B **216**(1989)360.
47. J. A. Casas, A. Ibarra, Nucl. Phys. B **618**(2001)171.
48. A.G. Akeroyd and F. Mahmoudi. JHEP **10**(2010)038.